

## Hardware-in-the-Loop Simulation and Control Design for Autonomous Free-Running Ship Models

Awanish Chandra Dubey\* and V. Anantha Subramanian

*Department of Ocean Engineering, Indian Institute of Technology Madras, Chennai - 600 036 , India*

*\*E-mail: wanish.dubey@gmail.com*

### ABSTRACT

This paper presents an hardware-in-the-loop (HIL) simulation system tool to test and validate an autonomous free running model system for ship hydrodynamic studies with a view to verification of the code, the control logic and system peripherals. The computer simulation of the plant model in real-time computer does not require the actual physical system and reduces the development cost and time for control design and testing purposes. The HIL system includes: the actual programmable embedded controller along with peripherals and a plant model virtually simulated in a real-time computer. With regard to ship controller design for ship model testing, this study describes a plant model for surge and a Nomoto first order steering dynamics, both implemented using Simulink software suit. The surge model captures a quasi-steady state relationship between surge speed and the propeller rpms, obtained from simple forward speed towing tank tests or derived analytically. The Nomoto first order steering dynamics is obtained by performing the standard turning circle test at model scale. The control logic obtained is embedded in a NI-cRIO based controller. The surge and steering dynamics models are used to design a proportional-derivative controller and an LQR controller. The controller runs a Linux based real-time operating system programmed using LabVIEW software. The HIL simulation tool allows for the emulation of standard ship hydrodynamic tests consisting of straight line, turning circle and zigzag to validate the combined system performance, prior to actual for use in the autonomous free-running tests.

**Keywords:** HIL; Proportional-derivative control; LQR; Nomoto model; LabVIEW; TCP/IP

### 1. INTRODUCTION

Studies on maneuverability and steering control and design of autopilots require physical simulations in laboratory environment. Even with the availability of computational tools for simulations, it is necessary to validate the results through physical models. The standards on maneuvering requirements of vessels set by regulatory bodies such as the International Maritime Organisation (IMO) also make it necessary to validate the maneuvering capability through simulations and physical experiments on scaled down models. The ship dynamics in 6-DOF is determined from the first principle using Newtonian Mechanics<sup>1</sup>. The assessments based on nonlinear and coupled hydrodynamics coefficients involved in the equations of motion are fairly complex to obtain through experimental or numerical techniques<sup>2-5</sup>. The 6-DOF motion is decoupled into two sets namely, the vertical plane motions which include roll-pitch and heave sub-system and horizontal motions which include the surge-sway-yaw sub-system. The latter helps in the study of maneuvering of ship and surface vehicles<sup>6</sup>. Nomoto presented a simplified steering model of a ship for designing autopilots based on input-output based transfer function<sup>7</sup>. The coefficients of Nomoto transfer-function is obtained using self-propelled scaled down ship models by

performing free running tests and standard maneuvers. Based on the Nomoto transfer function, different steering control models are evaluated for designing the autopilot system. However, steering control design needs rigorous testing and it is therefore necessary to conduct simulation before wet trials. Development of a simulation software helps in designing and tuning the controller based on results from free-running model tests. On the other hand, Hardware-in-the-Loop (HIL) helps in debugging, testing and validating the peripherals along with the program developed for the actual controller. The first use of analog HIL was to simulate the airplane flight by a pilot<sup>8</sup>. Later the digital HIL became popular in field of Aircraft and aerospace<sup>9,10</sup> industries, vehicle systems<sup>11,12</sup>, power systems<sup>13</sup>, robotics<sup>14</sup> and marine systems<sup>15,16</sup>. The technique is to place the hardware in the loop with the plant model running in real-time computer and study the motion behaviour of the model for various inputs. The HIL simulation allows to test and compare the responses of different control design models without the need for physical simulation in each case. HIL testing for the controller before implementation in a real system effectively reduces development cost as well as the risk of potential hazards in real physical testing<sup>17-21</sup>.

The organisation of this study is as follows: The second section introduces system dynamics in the horizontal plane motions and the first order system for a vessel, including description of the PD and LQR controller design for heading

control, The next section discusses the HIL system architecture and the actual hardware components, followed by HIL simulation results and conclusion from the studies.

## 2. SYSTEM DYNAMICS AND CONTROL DESIGN

### 2.1 Surge Lookup Table

This is a quasi-steady-state model relating propeller rotation rate with vessel surge speed. The resulting curve that relates these variables can be obtained either analytically or, more reliably, by performing careful tests on a scaled down model in a towing tank. In all cases the final validation is required through physical model tests. The model is prepared with BLDC motor and controls and connected to the propeller through a shaft. The tests are fairly straight-forward and consist of revving the propeller to different steady rotational speeds and noting the steady speed achieved in each case. The model tests are performed at given operating speed and hence the lookup table which includes the given operating speed is sufficient for the surge model. Figure 1 shows the obtained results. A polynomial curve gives the relationship between propeller rpm and speed and is the input for the HIL simulation.

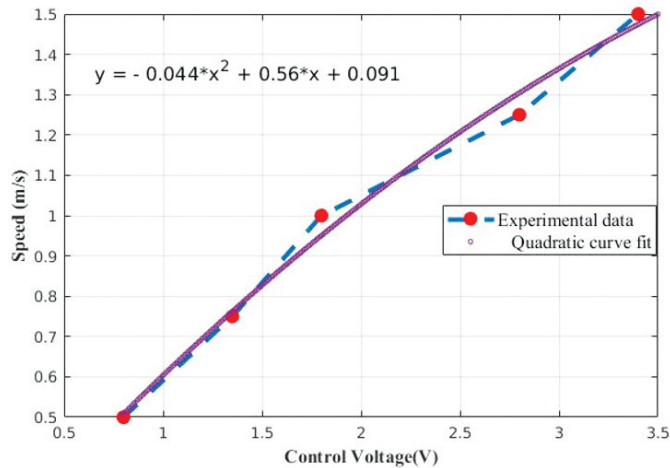


Figure 1. Surge model: speed vs control voltage curve.

### 2.2 Yaw Sub-system

The coupled nonlinear differential equations of motion in 6-DOF are derived using Newton-Euler equations. For our purposes it is sufficient to consider the equations of motion that describe the motion in the horizontal plane, yielding the equations<sup>1</sup>:

$$\begin{aligned} m[\dot{u} - vr - x_g r^2 - y_g \dot{r}] &= X \\ m[\dot{v} - ur - y_g r^2 - x_g \dot{r}] &= Y \\ I_z \dot{r} + m[x_g(\dot{v} + ur) - y_g(\dot{u} - vr)] &= N \end{aligned} \quad (1)$$

where  $m$  is the mass of the ship model,  $u$  is the surge velocity in the x-direction,  $v$  is the sway velocity in the y-direction,  $r$  is the yaw rate,  $I_z$  is the moment of inertia about the z-axis,  $x_g$  and  $y_g$  location of the centre of gravity,  $X$  indicates surge force,  $Y$  indicates sway force, and  $N$  represents the yaw moment. Under the assumption of constant surge speed and straight line maneuver, the above equation further reduces to

the sway and yaw equations, given by:

$$\begin{aligned} m[\dot{v} - u_0 r - y_g r^2 - x_g \dot{r}] &= Y \\ I_z \dot{r} + m[x_g(\dot{v} + ur) - y_g(\dot{u}_0 - vr)] &= N \end{aligned} \quad (2)$$

where

$$\begin{aligned} Y &= Y(v, r, \delta, \dot{v}, \dot{r}) \\ N &= N(v, r, \delta, \dot{v}, \dot{r}) \end{aligned} \quad (3)$$

and  $\delta$  is the rudder deflection.

In state-space form, the linearised maneuvering equations about the surge speed of 0.75 m/s can be written as:

$$\begin{bmatrix} m - Y_v & mx_g - Y_r \\ mx_g - N_v & I_z - N_r \end{bmatrix} \begin{bmatrix} \dot{v} \\ \dot{r} \end{bmatrix} = \begin{bmatrix} Y_v & Y_r - m \\ N_v & N_r - mx_g \end{bmatrix} \begin{bmatrix} v \\ r \end{bmatrix} + \begin{bmatrix} Y_\delta \\ N_\delta \end{bmatrix} \quad (4)$$

$Y_v$  and  $N_v$  are the added mass and added mass moment of inertia respectively.  $N_v$ ,  $Y_r$ ,  $Y_v$ ,  $Y_r$ ,  $N_v$ ,  $N_r$  and  $Y_\delta$ ,  $N_\delta$  are the damping coefficients and hydrodynamic derivatives related to rudder, respectively.

## 3. INPUT-OUTPUT BASED FIRST ORDER NOMOTO MODEL

The first order Nomoto model is derived from the linearised maneuvering model. Applying Laplace transforms to both sides of Eqn (4) and simplifying yields

$$\frac{\dot{r}}{\delta}(s) = \frac{K(1 + T_3 s)}{(1 + T_1 s)(1 + T_2 s)} \quad (5)$$

where  $T_1$  and  $T_2$  are the indices of stability on course and quick response in steering respectively,  $T_3$  represents the contribution of steering speed in initiating a turning motion and  $K$  is an index of turning ability<sup>7</sup>. The effective time constant is defined as,  $T = T_1 + T_2 + T_3$  where  $T$  can be estimated based on certain types of maneuvers such as turning circle of zigzag tests<sup>7</sup>. The steering motions of the ship can be approximated by the first order Nomoto model given by:

$$T\ddot{\psi} + \dot{\psi} = K\delta \quad (6)$$

The Laplace transformation of the above equation can be represented as:

$$\frac{r}{\delta}(s) = \frac{K}{(1 + Ts)} \quad (7)$$

which using the relation  $r = \dot{\psi}$  can be rewritten as:

$$\frac{\Psi}{\delta}(s) = \frac{K}{s(1 + Ts)} \quad (8)$$

The values of parameter  $K$  and  $T$  can be calculated using various technique<sup>22,23</sup>. For our purposes, the values of  $K$  and  $T$  were obtained by conducting the standard turning circle test on a scaled down free running model of a candidate coastal research vessel subjected to a forward speed of 0.75 m/s in a wave basin facility as shown in Fig. 2. The details of the vessel particulars are given in Table 1. By setting the constant rudder deflection of 35 degrees at forward speed the model achieves a constant yaw rate as shown in Fig. 3. By definition the settling time  $T_s$  is the time required to reach 98 % of the stable yaw rate; from the graph,  $T_s = 7.2$  s. The relation between pole location and settling time is<sup>24</sup>:

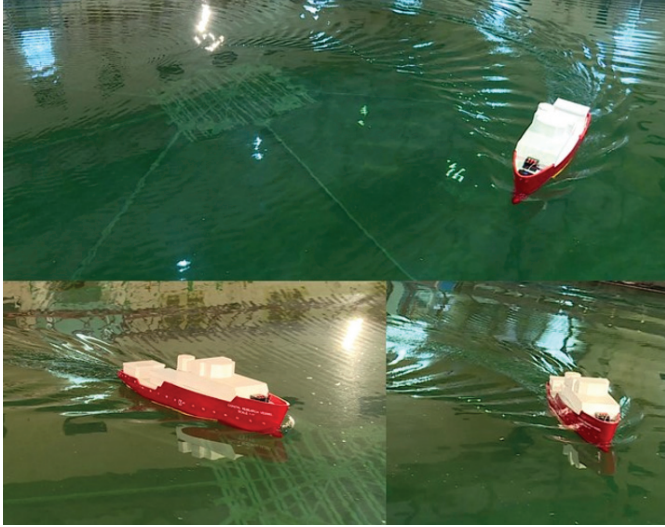


Figure 2. Ship model performing turning circle test in wave basin.

Table 1. Vessel particulars

Particular	Prototype	Model
Scale	1	17
Length overall, LOA	43 m	2529 mm
Length between perpendiculars, LBP	39 m	2294 mm
Length waterline, LWL	40.85 m	2403 mm
Breadth MLD	9.6 m	565 mm
Depth	3.7 m	218 mm
Design draft	2.5 m	147 mm
Displacement (Full Load Departure, LC03)	615.95t	121.95 kg
Design speed	12 kn	1.497 m/s
Propeller diameter	1300 mm	76.5 mm
Block Coefficient, C <sub>b</sub>		0.614
Froude number, F <sub>n</sub>		0.308

$$T_s \approx \frac{4}{a} \quad (9)$$

At the settling time, the yaw rate is -9.02 degrees per second and  $a$ , the pole location of the transfer function takes the value 0.56 rad/s.

The values obtained were  $K = 0.212$  and  $T = 1.785$ .

The equivalent state space representation of the first order system is:

$$\begin{bmatrix} \dot{\psi} \\ \dot{r} \end{bmatrix} = \begin{bmatrix} 0 & 1 \\ 0 & -\frac{1}{T} \end{bmatrix} \begin{bmatrix} \psi \\ r \end{bmatrix} + \begin{bmatrix} 0 \\ -\frac{K}{T} \end{bmatrix} \delta \quad (10)$$

$$y = \begin{bmatrix} 1 & 0 \end{bmatrix} \begin{bmatrix} \psi \\ r \end{bmatrix}$$

#### 4. STEERING CONTROL DESIGN

The control objective is to ensure that the vessel keeps a desired course despite external disturbances acting on it. The

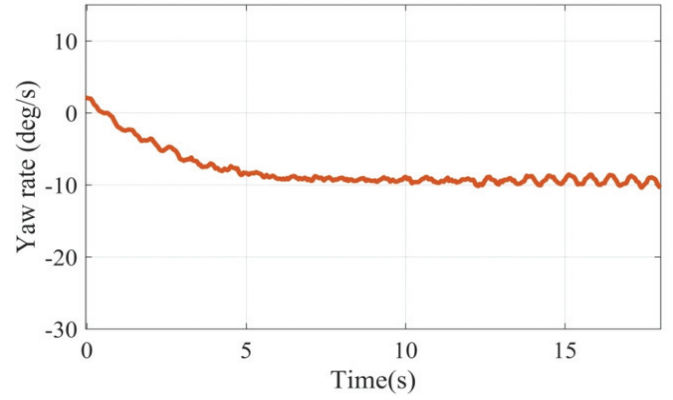


Figure 3. Yaw rate plot obtained from turning circle test.

steering control should drive the error  $e$  defined as  $\psi_d - \psi$  to zero at given surge speed (0.75 m/s), where  $\psi$  and  $\psi_d$  are the current heading angle and the set desired heading angle, respectively. In the scaled down laboratory tests these angles are measured on an on-board measurement device named motion reference unit (MRU). The control logic of the two control options, namely the PD controller and the LQR controller are as follows:

*PD Controller:* A Proportional-Derivative (PD) controller was designed using a standard frequency-domain approach, yielding the control law

$$\delta_r = K_p (\psi_d - \psi) - K_d \dot{\psi} \quad (11)$$

$$G(s) = \frac{K}{s(1+Ts)} \quad (12)$$

$$\frac{Y(s)}{R(s)} = \frac{G(s)H(s)}{1+G(s)(Hs)}$$

$$\text{where } H(s) = K_p + K_d s \quad (13)$$

$$\frac{Y(s)}{R(s)} = \frac{\frac{K}{s(1+Ts)}(K_p + K_d s)}{1 + \frac{K}{s(1+Ts)} * (K_p + K_d s)}$$

which yields the characteristic equation as:

$$Ts^2 + (1+KK_d)s + KK_p = 0 \quad (14)$$

Comparing the Eqn (14) with characteristic equation of the standard second order system

$$TF = \frac{\omega_n^2}{s^2 + 2\zeta\omega_n s + \omega_n^2} \quad (15)$$

where  $\omega_n$  is the natural frequency of the system and  $\zeta$  is the damping associated with it. The comparison yields the value of  $\omega_n$  and  $\zeta$  in terms of  $K_p$  and  $K_d$  as given below. In practice, for such a system the choice of  $\omega_n$  lies between 0.1-0.5 rad/s and the value of  $\zeta$  between 0.5-0.7<sup>25</sup>. The values of  $K_p$  and  $K_d$  are calculated by using following relation:

$$\omega_n^2 = \frac{K_p K}{T} \quad (16)$$

$$2\zeta\omega_n = \frac{1+KK_d}{T}$$

**LQR Controller:** For comparison purposes, a state feedback control law was designed using a Linear Quadratic Regulator (LQR) approach.

By conducting a turning circle test with a convenient rudder angle and measuring the steady yaw rate, one obtains the first order model transformed into state-space as given in Eqn. (9). The optimal LQR problem is defined more generally and consists of finding the control input that minimises.

$$J_{LQR} = \int_0^{\infty} x(t)'Qx(t) + \rho u(t)Ru(t)dt \quad (17)$$

where  $x$  is the state vector,  $u$  represents the control vector and  $Q$  and  $R$  are weighing matrices.

Under the assumption that system is controllable and observable, the solution to the above minimisation problem yields a stabilising state-feedback control law as  $u = -K_l(x - x_d)$ .

The closed loop dynamics<sup>26</sup> is then written as:

$$\dot{x} = (A - BK_l)x + BK_lx_d \quad (18)$$

$K_l$  is the feedback gain matrix,  $x_d$  represents the desired heading and serves as an external input to the closed-loop system, and  $A = \begin{bmatrix} 0 & 1 \\ 0 & -\frac{1}{T} \end{bmatrix}$ ,  $B = \begin{bmatrix} 0 \\ -\frac{K}{T} \end{bmatrix}$ .

The solution to the minimisation of cost function  $J_{LQR}$  is obtained by solving the Algebraic Riccati Equation given as:

$$PA + A^T P + Q - PBR^{-1}B^T P = 0 \quad (19)$$

And the gain is computed as:

$$K = R^{-1}B^T P \quad (20)$$

The value of  $Q \geq 0$  and  $R > 0$  are used to tune the controller gains by using the inbuilt function  $lqr(A, B, Q, R)$  in MATLAB, which assures that the bandwidth of the closed loop system lies well within the natural bandwidth of the actuators. Figure 4 shows the Simulink block diagrams for the control system with PID and LQR control. Figure 5 compares the responses of the close loop systems for the two types of controllers.

**5. HIL SYSTEM ARCHITECTURE**

This section is the focal point of the paper In what follows we describe the architecture of the HIL system and its implementation.

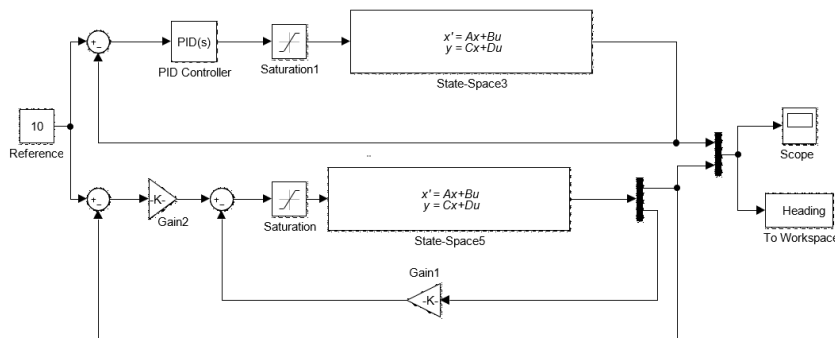


Figure 4. Simulink block for the comparison of PIPID and LQR controller.

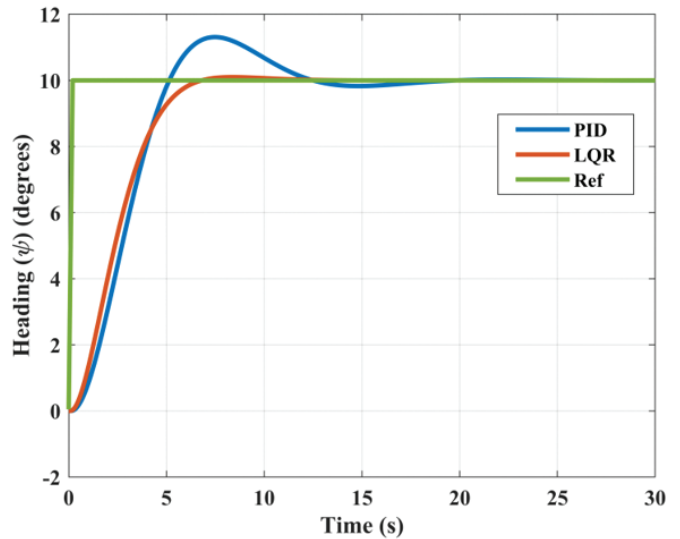


Figure 5. Comparison of PID and LQR responses in simulation.

The architecture of the HIL system consists of two parts: a simulated plant model and the actual embedded controller along with hardware components. Figure 6 shows the rudder and propeller interfaced with the hardware and explains the complete HIL architecture for the simulation of the free running ship model to perform definitive maneuvering tests. The real-time embedded system along with the hardware and peripherals are tested and validated using the HIL simulation. The HIL simulation assigns input commands to the real controller from a computer running the graphical user interface (GUI). As per the assigned command, the real controller generates the actuator input signals and transfers it to the plant model simulated in the real-time computer. The solution from the dynamics of the plant model accordingly generates the simulated sensor output signals. The simulated sensor output signal is the feedback to the actual embedded controller for generating the error signal for the PID or LQR controller. The PID or LQR controller generates the actuator signal which goes back to the simulated plant model as the rudder input and forces the system dynamics.

**5.1 Hardware Components**

The electronic hardware required for actuating the propeller and rudder includes the main controller, the I/O module and stepper module<sup>27</sup>, interfaced to facilitate the execution of the HIL simulation.

**Processor:** The cRIO9064 from National Instruments as shown in Fig. 7(a), is the main controller which is ideal for advanced control and monitoring applications. It features an FPGA and a Linux based real-time processor. The clock frequency is 667 MHz with 512 MB DRAM and 1 GB storage. The main controller offers a different types of connectivity ports, including two Ethernet, one USB host, one USB device, and one serial<sup>28</sup>. The Wi-Fi router connected to the Ethernet port provides wireless connectivity with the base station. The MRU sensor connected to the

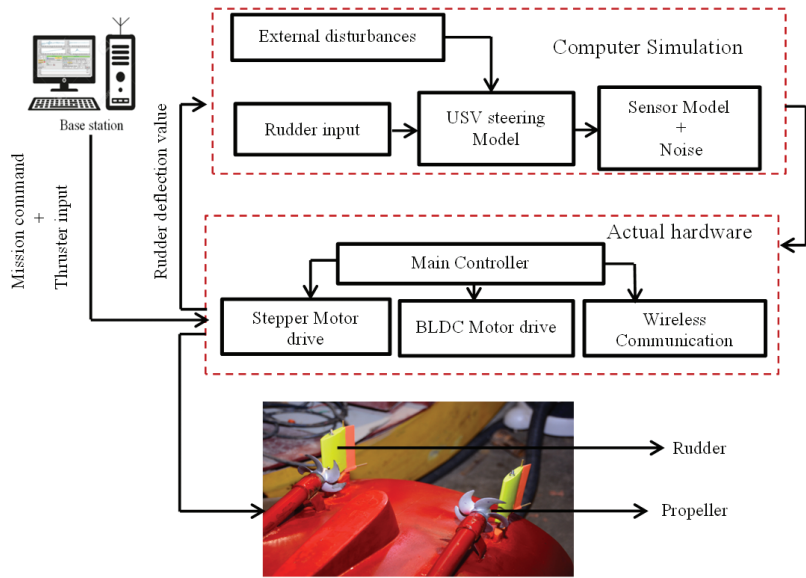


Figure 6. HIL architecture for the candidate ship model – coastal research vessel model on scale 1:17.

main controller through a serial (RS-232) port acquires motion data, which in turn is stored in the USB flash drive connected to the USB port of the main controller.

*I/O Module:* The NI-9381 is a general I/O module to interface peripherals with digital and analog I/O. The analog circuitry on the NI-9381 as shown in Fig. 7(b), is a multiplexed architecture that shares a single timing engine. The logic signal

are generated in the digital I/O pins to switch the controls of the BLDC drive circuit. The analog output of the I/O module controls the rpm of the motor.

*Stepper module:* The stepper motor for rudder control is interfaced with the main controller through NI9512 as shown in Fig. 7 (c), which provides stepper drive interface signals, compares position provides direct connectivity to the P7000 series stepper drives. The NI9512 processor runs the spline interpolation step generation algorithm to produce resulting smoother stepper motion control. All the components are assembled in an IP-66 enclosure in the circuit as shown in Fig. 7(d).

*Communication:* The communication between the simulated plant model and the actual embedded controller is through TCP/IP. The TCP/IP blocks configuration in Simulink and LabVIEW send and receive data. The actual hardware works as a server and the simulated plant model in computer works as a client.

6. SIMULATIONS AND RESULTS

The first Simulink based simulation results are the standard turning circle test and the zigzag test for the candidate coastal research vessel. See Fig. 8 (a) and (b) showing the control block diagrams, respectively. The simulation generates the control input based on experimentally obtained coefficients and no other hardware is involved. Figure 9(a) shows a simulation result of turning circle test, where a constant

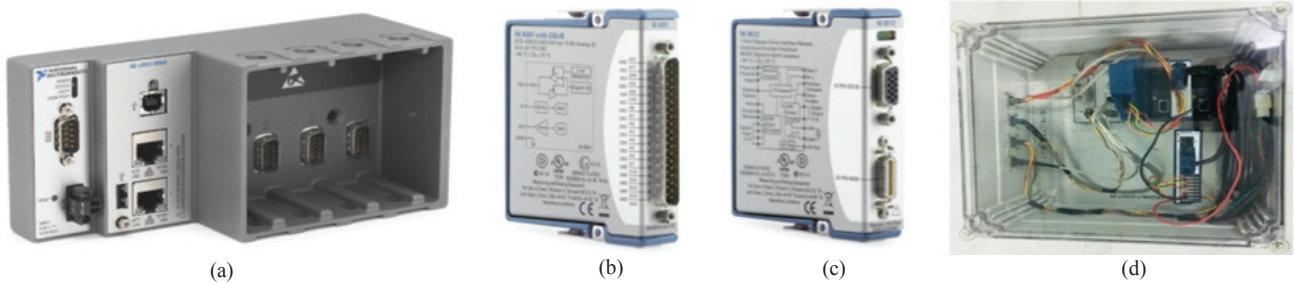


Figure 7. Hardware components used for HIL simulation (a) Main controller (cRIO), (b) I/O module, (c) Stepper motor module, and (d) assembled components.

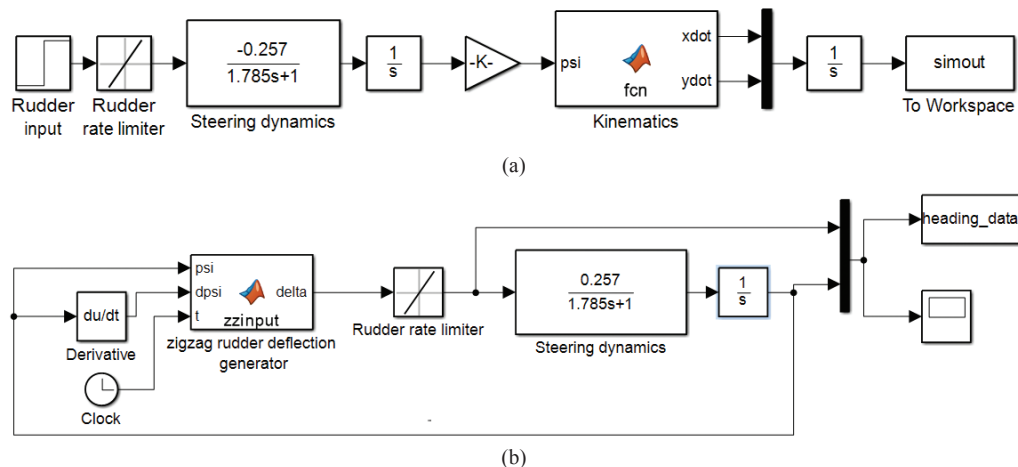


Figure 8. Simulink block diagram : (a) for turning circle test and (b) for zigzag test for the candidate coastal research vessel.

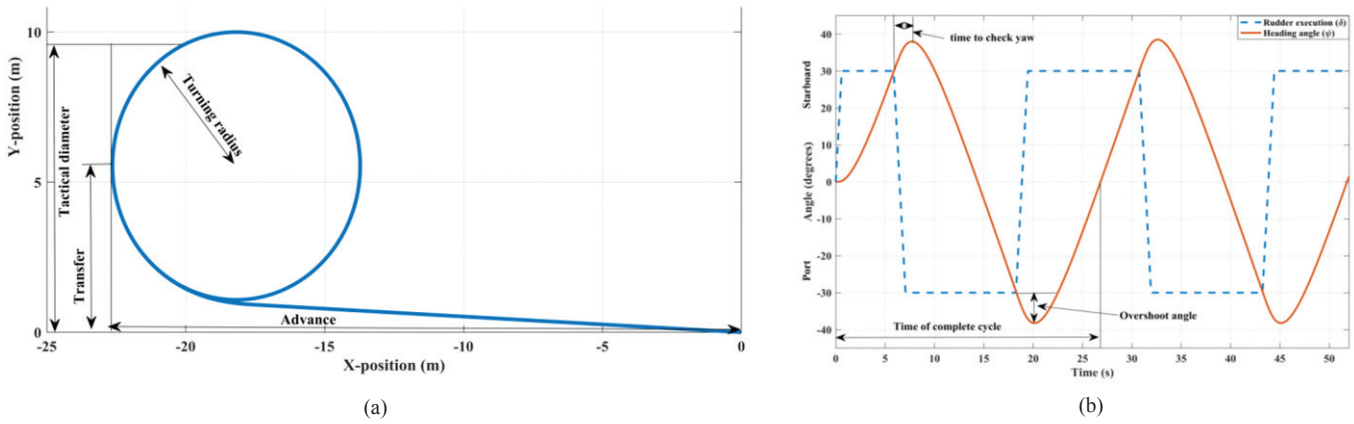


Figure 9. Simulation results: (a) turning circle test and (b) zigzag test for the candidate coastal research vessel model.

rudder angle (30 degrees) is set to execute circular path, and the maneuvering parameters such as tactical diameter, turning radius and transfer distance are measured. For the candidate coastal research vessel of length 2.2 m, the tactical diameter is 4.2 times the ship length is and the turning circle diameter is approximately 4 times the ship length.

These are typical characteristics of a small vessel. The zigzag simulation helps to assess the rudder effectiveness by calculating the initial turning time, overshoot angle when rudder is put to the opposite side and the time taken to complete one cycle. The simulation result obtained from the zigzag maneuver gives the initial turning time, (6s on model scale), overshoot angle 8.2 degrees and time for one complete cycle (26s on model scale), see Fig. 9(b). The simulated response of the turning circle is compared with the response obtained from physical model test as shown in Fig. 10. The error between the measured and simulated yaw rate value w.r.t. the measured value is approximately 10% .

To summarize, the HIL simulation effectively gives the ship maneuvering characteristics carried out for different command inputs for the plant model simulation from Simulink. This plant model receives the rudder control input from the real-time controller (runs LabVIEW) over TCP/IP communication, see Fig. 11. The “TCP/IP Client Receive” block in Simulink receives the control input and applies it to the plant model. Solving the equation for dynamics of the system generates the heading angle response. The sampling rate of the whole HIL simulation is fixed at 0.042s

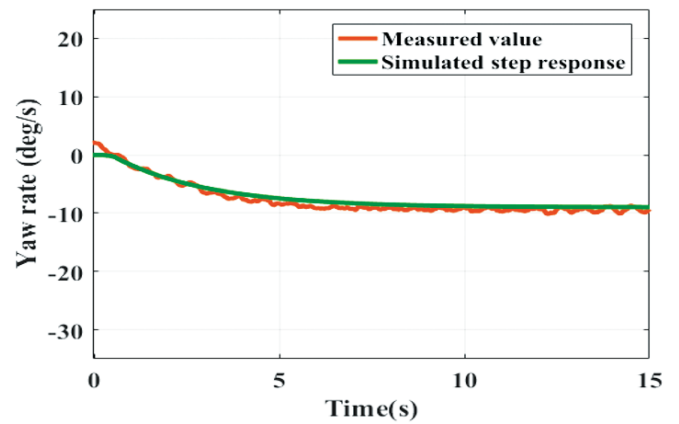


Figure 10. Comparison of experimental and simulated data of open loop response.

to synchronize with the sampling rate of the motion sensor. The TCP/IP which runs the LabVIEW program transfers the heading angle response to the actual embedded controller, and generates the control input for the plant model. The LabVIEW based GUI for HIL simulation (see Fig. 12) facilitates choice of different control inputs. The control inputs available on the GUI are: i) rudder control: allows the user to set the rudder deflection manually. ii) open/close loop: allows the user to set the model in autopilot mode to follow the desired heading. iii) zigzag: which allows to perform the zigzag maneuver test.

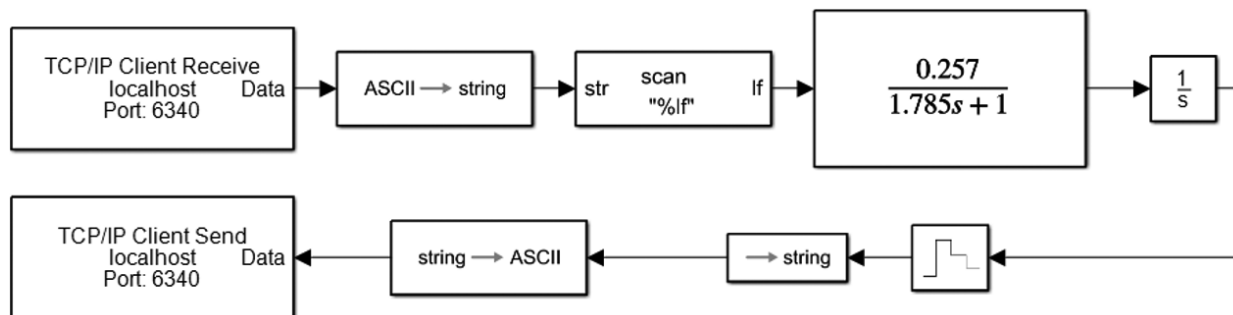


Figure 11. Simulink block diagram for HIL simulation.

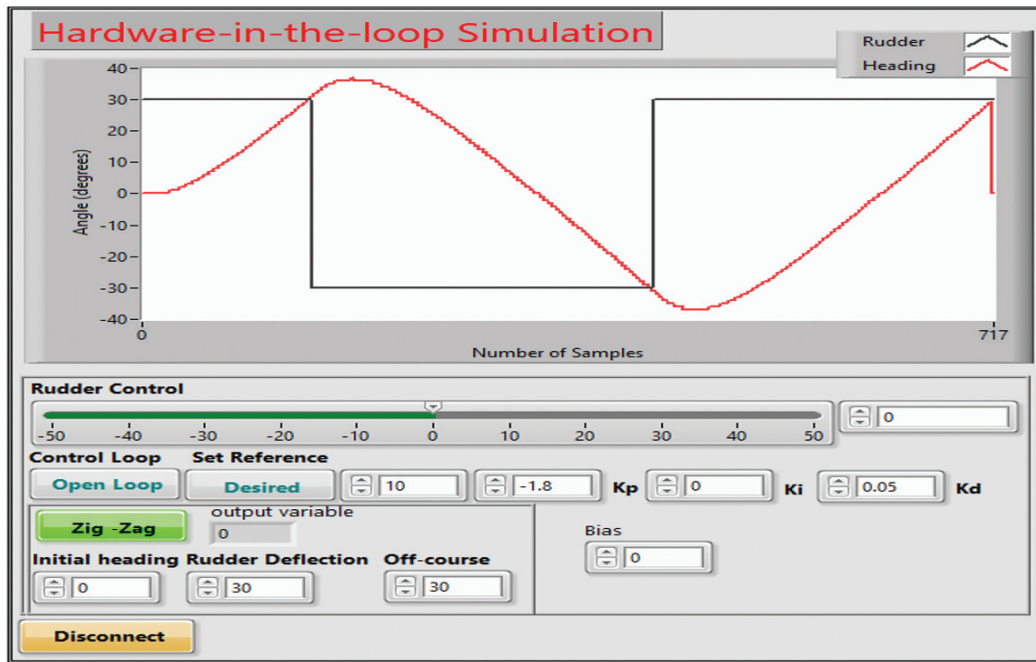


Figure 12. LabVIEW based GUGUI for HIL simulation.

## 7. CONCLUSIONS

This study reported the design and development of a Hardware-in-the-Loop simulation platform with illustration of the development and demonstration as applied to a candidate coastal research vessel in a laboratory scale model and development is pivotal for design of the heading control for performing very important hydrodynamic tests for maneuvering studies and quantifying the ability for turning and control. The HIL platform is developed on LabVIEW and Simulink platform along with embedded controller and peripherals and communicates over TCP/IP. The HIL simulation provides a platform to test and analyze different control schemes to perform maneuvering tests for the ship model. The results are of great value in assessing the maneuvering characteristics of the prototype vessel in view of stringent requirements by regulations. The use of HIL saves the cost, reduces time and effort of performing standard maneuvering tests. The HIL provides a successful testing platform prior to extension of work to standard maneuvering tests where the controller provides as a direct plug and play in physical simulations.

## REFERENCES

1. Fossen, Thor I. Handbook of marine craft hydrodynamics and motion control. John Wiley & Sons, 2011.
2. Skjetne, R.; Smogeli, Ø. & Fossen, T.I. Modeling, identification, and adaptive maneuvering of Cybership II: A complete design with experiments. *In Proceedings of the IFAC 2004*, **37**(10), 203-208. doi: 10.1016/S1474-6670(17)31732-9
3. Åström, K. J. & Källström, C. G. Identification of ship steering dynamics, *Automatica*, 1976, **12**(1), 9-22, doi: 10.1016/0005-1098(76)90064-9.
4. Qin, Y., & Zhang, L., Parametric identification of ships maneuvering motion based on Kalman filter algorithm, *In Proceedings of the Mechatronics and Automatic Control Systems*, Springer, 2014, 107-114.
5. Perera, L.P.; Oliveira P. & Soares C.G. System identification of nonlinear vessel steering, *J. Offshore Mech. Arctic Eng.*, 2015, **137**(3), 79-88. doi: 10.1115/1.4029826.
6. Skjetne, R.; Smogeli, Ø.N. & Fossen, T.I. A nonlinear ship manoeuvring model: Identification and adaptive control with experiments for a model ship. *Modelling, Identification and Control*, 2004, **25**(1), 3-27. doi: 10.4173/mic.2004.1.1.
7. Nomoto, K. & Taguchi, K.H.S. On the steering quality of ships. *International Shipbuilding Progress*, 1958, **4**(2), 354-370.
8. Isermann, R. & Schaffnit, J. & Sinsel, S. Hardware-in-the-loop simulation for the design and testing of engine-control systems. *Control Engineering Practice*, 1999 **7**(5), 643-653. doi: 10.1016/S0967-0661(98)00205-6
9. Karpenko, M. & Sepehri, N. Hardware-in-the-loop simulator for research on fault tolerant control of electrohydraulic flight control systems, *In Proceedings of the American Control Conference Minneapolis, MN, 2006*. doi: 10.1109/ACC.2006.1657454.
10. Spangenberg, H. & Friehe, H. Hardware-in-the-loop simulation with flight control actuators. *In AIAA Modeling and Simulation Technologies Conference and Exhibit 2005*, San Francisco, CA,
11. Güvenç, B.A.; Güvenç, L. & Karama, S. Robust yaw stability controller design and hardware-in-the-loop testing for a road vehicle. *IEEE Trans. Vehicular Technol.*, 2009, **58**(2), 555-571. doi: 10.1109/TVT.2008.925312.

12. Palladino, A.; Fiengo, G. & Lanzo, D. A portable hardware-in-the-loop (HIL) device for automotive diagnostic control systems. *ISA Transaction*, 2012, **51**(1), 229–236.  
doi: 10.1016/j.isatra.2011.10.009
13. Li, H.; Steurer, M.; Shi, K.L.; Woodruff, S. & Zhang, D. Development of a unified design, test, and research platform for wind energy systems based on hardware-in-the-loop real-time simulation. *IEEE Trans. Industrial Electron.*, 2006, **53**(4), 1144–1151.  
doi: 10.1109/TIE.2006.878319.
14. Martin, A. & Emami, M.R. Dynamic load emulation in hardware in-the-loop simulation of robot manipulators. *IEEE Trans. Industrial Electron.*, 2011, **58**(7), 2980–2987.  
doi: 10.1109/TIE.2010.2072890
15. Johansen, T.A.; Fossen, T.I. & Vik, B. Hardware-in-the-loop testing of DP systems. *In Proceedings of the Dynamic Positioning Conference*, 2005.
16. Hwang A.; S. Yoon; T. Kim; D. Kwon; C. Choi and H. Cho, Verification of unmanned underwater vehicle with velocity over 10 knots guidance control system based on hardware in the loop simulation. *In Proceedings of the OCEANS 2009*, IEEE, 1-5,  
doi: 10.23919/OCEANS.2009.5422227
17. Mastebe, O.; Kumile, C.M. & Tlale, N.S. A review of virtual simulators for autonomous underwater vehicles (AUVs). *In Proceedings of the IFAC Proceedings 2008*, **41**(1), 31-37.  
doi: 10.3182/20080408-3-IE-4914.00007
18. Woolsey, M. & Jarnagin, R. Design, implementation, and refinement of a hardware-in-the-loop simulator for a hovering AUV. *In Proceedings of the OCEANS 2012*, IEEE, 1-4.  
doi: 10.1109/OCEANS.2012.6404862.
19. Marouani, K.; Guendouz, H.; Tabbache, B.; Khoucha, F. & Kheloui, A, Experimental investigation of an emulator Hardware In the Loop for electric naval propulsion system. *In Proceedings of the 21st Mediterranean Conference on Control and Automation IEEE*, 125-130.  
doi: 10.1109/MED.2013.6608709
20. Bao, D.; Yang, R.; Ma, Y. & Clement, B. Hardware-in-the-loop simulation applied to AUV control. *In Proceedings of the Chinese Automation Congress (CAC)*, 2018, China, 1009-1013.  
doi: 10.1109/CAC.2018.8623733
21. Chaudhuri, S.; Venkatachalam, G. & Prabhakar, M. Hardware in loop simulation for missile guidance and control systems. *Def. Sci. J.*, 1997 **47**(3), 343-357.  
doi: 10.14429/dsj.47.4016
22. Desa, E.; Maurya, P. K.; Pereira, A.; Pascoal, A. M.; Prabhudesai, R. G.; Mascarenhas, A. & Prabhudesai, S. A small autonomous surface vehicle for ocean color remote sensing. *IEEE J. Oceanic Eng.*, 2007, **32**(2), 353-364.  
doi: 10.1109/JOE.2007.893688.
23. Maurya, P.; Desa, E.; Pascoal, A.; Barros, E.; Navelkar, G.; Madhan, R. & Naroji, S. Control of the Maya AUV in the vertical and horizontal planes: Theory and practical results. *In Proceedings of the 7th IFAC Conference on Manoeuvring and Control of Marine Craft 2006*.
24. Nise, N. S. *Control Systems Engineering*, John Wiley & Sons, 2007.
25. Fryxell, D.; Oliveira, P.; Pascoal, A. & Silvestre, C. An integrated approach to the design and analysis of navigation, guidance and control systems for AUVs. *In Proceedings of the IEEE Symposium on Autonomous Underwater Vehicle Technology*, 1995, 208-217,  
doi: 10.1109/AUV.1994.518627.
26. Hespanha, J. P. *Lecture notes on LQR/LQG controller design*, 2005.
27. Dubey A.C.; Subramanian V.A. & Kumar V.J. Embedded System Design for Autonomous Unmanned Surface Vehicles in Laboratory Environment. *In Proceedings of the Fourth International Conference in Ocean Engineering (ICOE) 2018*, **22**, 465-477  
doi:10.1007/978-981-13-3119-0\_27
28. National Instruments, website address: <http://www.ni.com>. (Accessed on 20 March 2020).

## CONTRIBUTORS

**Mr Awanish Chandra Dubey** received his MTech from Devi Ahilya Vishwavidyalaya University, in 2011. Currently pursuing his PhD in the Department of Ocean Engineering, IIT Madras. His research interest includes: control of unmanned marine vehicles, underwater localisation and navigation of underwater vehicle.

The author's contribution in the paper was design and implementation of control system and HIL system tool for the ship model testing. The contribution also includes the development of on-board instrumentation, interface of the peripherals with the main controller and model testing in the wave basin to obtain the steering dynamics for the candidate vessel.

**Prof. V. Anantha Subramanian** has been with the Department of Ocean Engineering, IIT Madras. His major area is naval architecture and ocean engineering with specialised interest in computational fluid dynamics applications, computer-aided ship design, ship hydrodynamics, design and testing and optimisation related to ships and floating bodies.

The author supported with his consistent guidance and his contribution in the paper was making and deciding strategies for the maneuvering tests in wave basin. Author also supported the entire required infrastructure to carry out the research and development work.